

Multi-electron giant dipole resonances of atoms in crossed electric and magnetic fields

S. ZÖLLNER¹(*), H.-D. MEYER¹(**) and P. SCHMELCHER^{1,2}(***)

¹ *Theoretische Chemie, Physikalisch-Chemisches Institut, INF 229, Universität Heidelberg, 69120 Heidelberg, Germany*

² *Physikalisches Institut, Philosophenweg 12, Universität Heidelberg, 69120 Heidelberg, Germany*

PACS. 32.60.+i, 32.10.-f, 32.30.-r -

Abstract. – Multi-electron giant dipole resonances of atoms in crossed electric and magnetic fields are investigated. Stationary configurations corresponding to a highly symmetric arrangement of the electrons on a decentered circle are derived, and a normal-mode stability analysis is performed. A classification of the various modes, which are dominated either by the magnetic or Coulomb interactions, is provided. A six-dimensional wave-packet dynamical study, based on the MCTDH approach, is accomplished for the two-electron resonances, yielding in particular lifetimes of more than $0.1 \mu\text{s}$ for strong electric fields.

Introduction. – Atoms exposed to strong external fields have proven to be a persistent source of intriguing phenomena with major impact on a variety of other fields such as the quantum dynamics of finite systems or Laser spectroscopy of Rydberg atoms [1–3]. Focusing on crossed electric and magnetic fields, new configurations of the hydrogen atom, the so-called giant dipole states, were discovered in the nineties [4–6]. These states represent a new form of microscopic matter where the electron and proton are separated by large distances due to the presence of an electric field: There exists an outer potential well whose bound atomic states possess a huge electric dipole moment. The atomic wave function then resembles an oscillating barbell in contrast to the usual shell-like structure of the electronic states in field-free space. In refs. [7] the giant dipole states of Positronium have been investigated, thereby arriving at the conclusion that the decentered positron-electron configuration is a quasistable state, i.e., the matter-antimatter system could be prevented from annihilation for very large time scales up to several years. Recently, dipolar matter has also become of major interest in the context of ultracold atomic and molecular physics, such as dipolar quantum gases [8] or ultracold molecular Rydberg states [9].

In the present investigation we consider an N -electron atom (total mass M) where the electrons (m) and the nucleus, interacting via the Coulomb potential V , are subject to crossed electric and magnetic fields. The translational invariance yielding the conservation of the

(*) e-mail: sascha@tc.pci.uni-heidelberg.de

(**) e-mail: dieter@tc.pci.uni-heidelberg.de

(***) Corresponding author; e-mail: peter@tc.pci.uni-heidelberg.de

total canonical momentum in the absence of the fields is now lost, which manifests itself in the appearance of the coordinate-dependent vector potential. For homogeneous fields the conserved (total) pseudomomentum $\mathbf{K} = \sum_{i=0}^N \mathbf{k}_i$ with $\mathbf{k}_i = \mathbf{p}_i - e_i \mathbf{A}_i + e_i \mathbf{B} \times \mathbf{r}_i$, whose components commute due to the neutrality of the atom, is a conserved quantity associated with the center-of-mass (CM) motion of the atom [10–13]. It can be exploited to perform a so-called pseudoseparation of the CM motion. The latter was originally done [10–13] for a fixed gauge. It is only recently that gauge-independent pseudoseparations for one-electron [6] and many-electron systems [14] have been performed. The latter provided a generalized potential for the electronic motion, possessing major impact on the prediction of new structures and effects in crossed fields such as the decentered giant dipole states [6, 14]. Our starting point is the pseudo-separated Hamiltonian

$$\mathcal{H} = \frac{m}{2} \sum_{i=1}^N \dot{\mathbf{r}}_i^2 - \frac{1}{2M} \left(\sum_{i=1}^N m \dot{\mathbf{r}}_i \right)^2 + \frac{1}{2M} \left(\mathbf{K} - e\mathbf{B} \times \sum_i \mathbf{r}_i \right)^2 - e\mathbf{E} \cdot \sum_{i=1}^N \mathbf{r}_i + V, \quad (1)$$

where the first two terms and the last three terms represent the gauge-dependent kinetic energy of the electrons relative to the nucleus ($\dot{\mathbf{r}}_i = \dot{\mathbf{r}}_i(\{\mathbf{p}_j, \mathbf{A}(\mathbf{r}_j)\})$, $i, j = 1, \dots, N$) and the generalized gauge-independent potential, respectively. The potential contains, besides the Coulomb interaction V , Stark and diamagnetic interaction terms that are responsible for the existence of an outer well and bound giant dipole states for sufficiently strong (external and/or motional) electric fields in the one-electron case.

Little is known, however, about multi-electron giant dipole resonances (GDR) which are the subject of the present investigation: In Ref. [14] a naturally limited analytical investigation of the decentered two-electron configuration was performed. It provided evidence, but no final conclusion, on the existence of highly symmetric decentered resonances. In the following we derive the electronic configurations corresponding to the decentered N -electron giant dipole resonances. We classify the modes and investigate their stability. Moreover, a numerically exact six-dimensional wave-packet dynamical investigation of two-electron resonances will be performed, supplying valuable information on lower bounds of the lifetimes of the GDR.

Stationary decentered configurations. – With the gauge-independent generalized potential at hand, let us search for decentered stationary points, being candidates for configurations of GDR. Inspecting the generalized potential (see Eq. 1), it is natural to introduce the electronic center of mass (ECM) $\mathbf{R} = \frac{1}{N} \sum_{i=1}^N \mathbf{r}_i$ as a new coordinate. In addition, we choose $N-1$ vectors relative to the ECM, i.e., we decompose $\mathbf{r}_i =: \mathbf{R} + \mathbf{s}_i$, $i = 1, \dots, N-1$. Defining $Q = (\mathbf{R}, \mathbf{s}_1, \dots, \mathbf{s}_{N-1})^T$ we seek the stationary configuration

$$\frac{\partial \mathcal{V}}{\partial Q}(Q_0) = 0. \quad (2)$$

Employing the coordinate frame $\boldsymbol{\zeta} = \mathbf{B}/B$; $\boldsymbol{\eta} = \mathbf{K}'/K'$; $\boldsymbol{\xi} = \boldsymbol{\eta} \times \boldsymbol{\zeta}/|\boldsymbol{\eta} \times \boldsymbol{\zeta}|$ (where $\mathbf{K}' = \mathbf{K} + M\mathbf{E} \times \mathbf{B}/B^2$, and we assume $\angle(\mathbf{K}', \mathbf{B}) = 90^\circ$), one can show that there exist solutions that fulfill $|\mathbf{r}_i^{(0)}| \equiv |\mathbf{R}_0 + \mathbf{s}_i^{(0)}| =: r \forall i$ such that the ECM vector $\mathbf{R} = X\boldsymbol{\xi} + Y\boldsymbol{\eta} + Z\boldsymbol{\zeta}$ is aligned along the $\boldsymbol{\xi}$ axis, $\mathbf{R}_0 = (X_0, 0, 0)^T$, where the decentering coordinate X_0 satisfies

$$P_r(X_0) \equiv -\frac{NeK'B}{M} + \frac{(NeB)^2}{M} X_0 + NZe^2 \frac{X_0}{r^3} = 0. \quad (3)$$

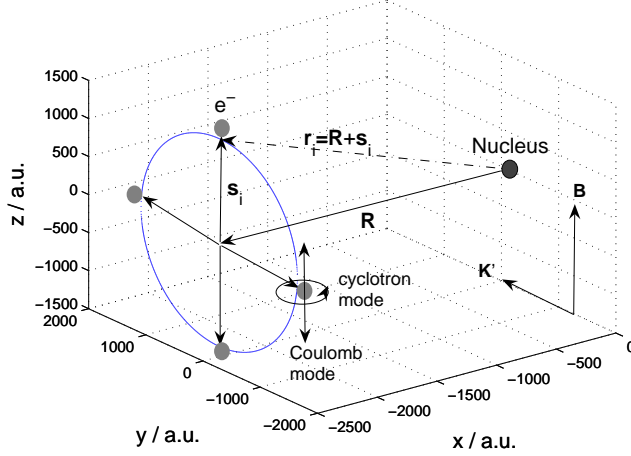


Figure 1 – A giant-dipole configuration for $N = 4$ electrons ($B = 10^{-4}$, $K = 2K_{\text{cr}}$). The ECM $\mathbf{R} = (X, 0, 0)$ is decentered, with the relative vectors \mathbf{s}_i confined to a circle as indicated. Also shown is the electronic vector relative to the nucleus $\mathbf{r}_i = \mathbf{R} + \mathbf{s}_i$. Typical motions for the cyclotron and Coulomb mode are indicated.

Moreover, the relative coordinates are arranged on a circle in the orthogonal complement, $\mathbf{s}_i = s(0, \cos \phi_i, \sin \phi_i)^T$. For symmetry reasons, we demand that all relative coordinates be distributed uniformly on that circle

$$\phi_k = \Phi_N k + \Delta, \quad \Phi_N \equiv 2\pi/N. \quad (4)$$

This procedure determines the decentered configuration only up to a global rotation by an angle $\Delta \in [0, 2\pi)$. However, it allows us to fix the ratios of $|X_0|$ and s, r

$$r = s \sqrt[3]{\frac{4N}{\sum_{k=1}^{N-1} (1/\sin \frac{\Phi_k}{2})}} =: \alpha_N s =: \tilde{\alpha}_N |X_0| \quad (5)$$

and thus to solve Eq. (3). The solutions are

$$X_0(K') = \frac{K'}{3NB} (2 \cos(\frac{\theta+2\pi}{3}) - 1)$$

where $\theta \equiv \arccos[2(K_{\text{cr}}/K')^3 - 1]$, provided that $K' \geq K_{\text{cr}} \equiv \frac{3N}{\tilde{\alpha}_N} \sqrt[3]{\frac{MB}{4}}$. For any B there is a critical value K_{cr} for K' at which the decentering sets in. Experimentally, the value of K' can be controlled via the strength of the external electric field.

To conclude, the stationary electronic vectors possess the orthogonal decomposition $\mathbf{r}_i = X\boldsymbol{\xi} + s(0, \cos \phi_i, \sin \phi_i)^T$ with the common decentering along $\boldsymbol{\xi}$. They are confined to a highly symmetric circular configuration perpendicular to $\boldsymbol{\xi}$. This circular configuration is determined up to an overall rotation Δ . A generic setup is sketched in Figure 1. The extremal solution exists only if the effective pseudomomentum K' exceeds some critical value given above. With increasing K' the decentering of the ECM becomes more pronounced.

Normal-mode analysis of N-electron giant dipole states. – We expect the decentered stationary configurations to be promising candidates for GDR with certain lifetimes. Preceding a numerical study, we first seek to obtain some insight into the local stability of the

extremal configurations. According to Ehrenfest's theorem, the expectation values $\langle Q \rangle(t)$ of a harmonic system obey the corresponding classical equations of motion. This suggests treating the problem within a normal-mode analysis.

The equations of motion are obtained in terms of the displacements $v(t) := Q(t) - Q_0$,

$$\ddot{v} = \omega \cdot \dot{v} + A \cdot v. \quad (6)$$

The antisymmetric $3N \times 3N$ cyclotron matrix ω contains the Lorentz force and the harmonic matrix A is built up essentially from the Hessian of the generalized potential. The solution of this system of differential equations is given by the span

$$v(t) = \sum_{\rho=1}^{6N} (v_{\rho} e^{\gamma_{\rho} t}) c_{\rho} \quad (v_{\rho} \in \mathbb{C}^{3N}; \gamma_{\rho}, c_{\rho} \in \mathbb{C}), \quad (7)$$

fulfilling the quadratic eigenvalue equation

$$(\gamma_{\rho}^2 I - \gamma_{\rho} \omega - A) v_{\rho} = 0, \quad (8)$$

I being the identity. Our stability analysis amounts to finding the complex eigenvalues $\gamma_{\rho} =: \Gamma_{\rho} + i\Omega_{\rho}$ (whose imaginary parts are frequencies of a vibration about a stable point, and whose real part corresponds to an instability), and the eigenvectors v_{ρ} . The above quadratic eigenvalue problem is solved by reducing it to the standard linear eigenvalue problem

$$\begin{pmatrix} 0 & I \\ A & \omega \end{pmatrix} u = \gamma u; \quad u \equiv \begin{pmatrix} v \\ \dot{v} \end{pmatrix}. \quad (9)$$

Every eigenpair (γ, v) of (8) with $\text{Im}\gamma \neq 0$ has a twin pair (γ^*, v^*) . Thus we treat the $6N$ modes as effectively $3N$ modes.

If one studies the behavior of the modes $\{\gamma_{\rho}(K; B)\}_{\rho}$ for different electron numbers N in the vertical configuration $\Delta = -\pi/2$, one observes that even though the patterns become increasingly rich and involved with larger N , there is a clear distinction between the character of the modes regarding their behavior as a function of K (and B), their order of magnitude and, more generally, their location in the complex plane. Based on our analysis, including the associated eigenvectors, we arrive at the following classification of the $3N$ eigenmodes:

- N so-called cyclotron modes corresponding to the cyclotron motion of the effective electronic particles. Their values are exclusively of the order of the cyclotron frequencies, $\gamma = i\Omega \sim i \frac{|e|B}{m}$, i.e., almost independent of K .
- N Coulomb modes corresponding to the inter-Coulombic motion, with dominating contributions from the harmonic matrix A . They fall off quickly with K , since the decentering $X_0(K)$ increases, and the Coulomb interaction weakens. As opposed to the cyclotron modes, the Coulomb motion takes places predominantly parallel to \mathbf{B} .
- 1 CM mode, roughly reflecting the cyclotron motion of the CM, $\Omega \sim \frac{NeB}{M}$.
- 1 zero mode ($\gamma_{\rho} = 0$) stemming from the rotational invariance of the saddle point with respect to the circular configuration (see Eq. 4)
- $N - 2$ modes termed decay modes in recognition of the fact that they are predominantly real. They are neither directly related to the cyclotron motion nor to the spectrum of A , and their slope is twice as steep as that of the Coulomb modes. Their absence for the case $N = 2$ is essentially why the two-electron system is locally stable.

A generic example for the spectrum is given in Fig. 2 for the case of $N = 4$ electrons. There are a few subtleties that go beyond the categorization suggested above. Without going

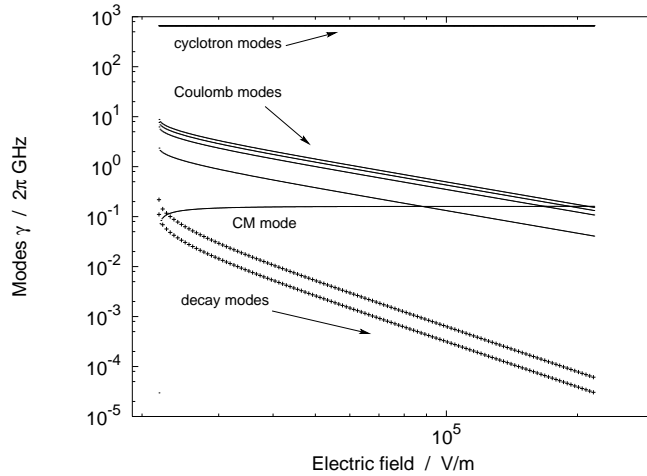


Figure 2 – Eigenmodes $\{\gamma_\rho\}_\rho$ for $N = 4$ electrons as a function of the electric field $E \equiv BK/M$, shown for the range $K/K_{\text{cr}} \in [1, 10]$ ($B = 10^{-4}$). Imaginary parts appear as solid lines, while points (+) are used for the real parts. – The top horizontal line represents four almost degenerate cyclotron modes. Below, the four Coulomb modes fall off quickly and intersect the CM mode (the nearly horizontal line about four orders below the cyclotron modes). There are two residual decay modes, whose slope is twice that of the Coulomb modes.

into the details, we mention that there are certain interactions among different mode types. Their principal causes are crossings between the CM mode and the decay modes (resulting in some striking deformations of the usual line pattern), and avoided crossings of the CM mode with at least some of the Coulomb modes. This may be taken as a hint for the different symmetry relations among the Coulombic and the decay modes.

Let us remark on the influence of the global rotations Δ . While the stationary character is not affected by a common rotation of the relative coordinates \mathbf{s}_i by an angle Δ on the circle, the dynamics differs. In order to see this dependence, we inspect the modes as a function of the rotation angle $\{\gamma_\rho(\Delta)\}$. Apart from an obvious symmetry—note that rotating by $\Phi_N = 2\pi/N$ gives an indistinguishable setup—we found that the Coulomb modes and the decay modes show a pronounced periodic change. For the case $N = 2$, we encounter an exceptional behavior whenever Δ comes close to $0 \bmod \pi$. One of the Coulomb modes then tends to zero, along the way turning real. In this respect, the local stability indicated above is applicable only outside the singular horizontal configuration $\Delta = 0$.

Wave-packet dynamical study. – We now turn to a numerical study of the two-electron system ($N = 2$). We emphasize that a six-dimensional resonance study is at the frontier of what is currently possible and requires a careful choice of the computational approach. This applies especially in view of the fact that our system is governed by dramatically different time scales (see below). Therefore we adopted the Multi-Configuration Time-Dependent Hartree (MCTDH) method [15, 16], a wave-packet propagation scheme known for its outstanding efficiency in high-dimensional settings. Its basic idea is to solve the time-dependent Schrödinger equation by expanding the wave function in a moderately sized time-dependent basis related to Hartree products. We stress that this approach is designed for distinguishable particles. Applying it to a fermionic system like ours finds its sole justification in the fact that the spatial

separation between the electrons is so large that they are virtually distinguishable.

Let us first point out how the computational method can be applied to our problem. There are essentially two conflicting types of motion and corresponding scales: perpendicular to the magnetic field, we have the magnetic length $R_B \sim 10^2$ a.u. (for the strong laboratory field strength $B = 10^{-4}$ a.u. we consider). For the Coulomb motion parallel to \mathbf{B} —expected to take place approximately in a harmonic potential—we can use the usual oscillator lengths $z_0 \equiv 1/\sqrt{m\omega_z}$ as an estimate. These are roughly on the order of 10^3 a.u. but increase with K (see above). Analogously, the anticipated time scales are $T_B = \frac{2\pi}{\omega_B} \stackrel{B=10^{-4}}{\simeq} 1.5$ ps for the cyclotronic motion and 1.5ns – 15ns for the Coulomb motion.

Within our numerical study we focus on the investigation of the stability of the giant dipole states by using the propagation of harmonic-oscillator wave packets initially localized at the extremal position. Relaxation techniques have been applied in order to improve the initially chosen wave packet. Moreover, following the evolution of wave packets with an initial displacement from the extremum, we tested the robustness of the resonances. For comparison, we also examine the decentered eigenvectors. The chosen parameter set is $K/K_{\text{cr}} \in \{1.1, 2.0, 10.0\}$ (we drop the prime here and in the following), which accounts for the cases of just above threshold, the medium range and the very large K regime. For simplicity, we first focus on the vertical configuration $\Delta = -\pi/2$. The propagation times are chosen in the regime of 50 – 100 ns; this includes many periods of the Coulomb modes and some 10,000 periods of the rapid cyclotron motion !

Very close to the critical point, e.g. $K = 1.1K_{\text{cr}}$, the observed motion is unstable for several degrees of freedom, specifically for those belonging to the relative vector $\mathbf{s}_{\perp} = (x, y)^T$ perpendicular to the magnetic field, on a time scale of 10^3 ps. Other modes are affected too via couplings. This is a general fact, but for $K = 1.1K_{\text{cr}}$ it is very pronounced, whereas it is suppressed for the time evolution in case of larger values of K due to the weaker Coulomb modes (see Fig. 2).

For K being twice its critical value, $K = 2K_{\text{cr}}$, the vertical configuration is virtually stable on a scale of $T \sim 10^4$ ps. As opposed to the case $K/K_{\text{cr}} = 1.1$, the instability is almost exclusively due to the relative motion in y . However, the response of the system upon displacing the initial wave packet in Z and z by 2,000 a.u. unveiled that x is rendered rather unstable. Hence the resonance is expected to be less robust, although its lifetime is not significantly reduced altogether. To illustrate the resonance character of the system, Fig. 3 gives an impression of the excitation spectrum, obtained via Fourier transformation of the auto-correlation function $c(t) := \langle \Psi_0 | e^{-iHt} \Psi_0 \rangle$. The ‘displaced state’ with $\langle z \rangle_0 = \langle Z \rangle_0 = 2,000$ a.u. produces a rather interesting excitation spectrum. The equidistant spacing of the peaks can be interpreted as a signature of harmonicity for both excited degrees of freedom (Z, z).

For $K = 10K_{\text{cr}}$, we find the system to be practically stable on the time scale $T = 10^5$ ps. The initial wave packet experiences only tiny deformations with respect to all degrees of freedom but z , showing some oscillatory behavior. However, those are still marginal compared to the spatial extension of the decentered state. As a result of our wave-packet dynamical study, we can conclude that the lifetimes of the GDR for sufficiently large K are beyond $0.1\mu\text{s}$.

To complete the discussion, let us touch on the effects of different circular configurations Δ of the GDR. As examples, we investigated both the supposedly unstable ‘horizontal configuration’ ($\Delta = 0$) and a ‘diagonal configuration’ ($\Delta = -\pi/4$), corresponding to different settings of the extremal relative coordinates $\mathbf{s}^{(0)}$. To sum up our findings, the horizontal configuration indeed adds an instability, which is discernible even for very high K , if less distinct. The diagonal configuration was partly unstable on a timescale comparable to that of the vertical

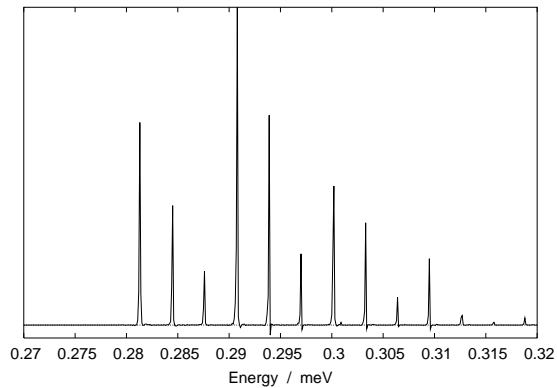


Figure 3 – Spectrum for $K/K_{cr} = 2$ for the excited initial state (displaced in Z, z).

case, $T \sim 10^4$ ps.

Conclusion and outlook. – Our investigation shows that atoms in crossed fields exhibit multi-electron giant dipole states with extraordinary lifetimes. These resonances constitute highly symmetric and exotic states of matter, where the electrons are strongly correlated and can, for laboratory field strengths, be separated from the nucleus (or positively charged core) by many thousand Bohr radii. An experimental preparation of the giant dipole states might employ the scheme suggested for single electrons [17]. The latter is based on the preparation of Rydberg states via Laser excitation, followed by a sequence of electric-field switches that carry the excited electrons to the decentered configuration. Preparing different initial Rydberg states, like circular ones, enhances the variety of accessible decentered states.

References

- [1] *Lecture Notes in Physics: Classical, Semiclassical and Quantum Dynamics in Atoms*, edited by H. FRIEDRICH and B. ECKHARDT, Vol. **485** (Springer) 1997.
- [2] *Atoms and Molecules in Strong External Fields*, edited by P. SCHMELCHER and W. SCHWEIZER (Plenum Press, New York) 1998.
- [3] *Rydberg Atoms* T.F. GALLAGHER, (Cambridge University Press) 1994.
- [4] I. DZYALOSHINSKII, *Phys. Lett. A*, **165** (1992) 69.
- [5] D. BAYE, N. CLERBAUX and M. VINCKE, *Phys. Lett. A*, **166** (1992) 135.
- [6] O. DIPPEL, P. SCHMELCHER and L.S. CEDERBAUM, *Phys. Rev. A*, **49** (1994) 4415.
- [7] J. ACKERMANN, J. SHERTZER and P. SCHMELCHER, *Phys. Rev. Lett.*, **78** (1997) 199; *Phys. Rev. A*, **58** (1998) 1129.
- [8] A. GRIESMAIER *et al.*, *Phys. Rev. Lett.*, **94** (2005) 160401.
- [9] C. H. GREENE, A. S. DICKINSON and H. R. SADEGHPOUR, *Phys. Rev. Lett.*, **85** (2000) 2458.
- [10] J.E. AVRON, I.W. HERBST and B. SIMON, *Ann. Phys. (NY)*, **114** (1978) 431.
- [11] B.R. JOHNSON, J.O. HIRSCHFELDER and K.H. YANG, *Rev. Mod. Phys.*, **55** (1983) 109.
- [12] H. HEROLD, H. RUDER and G. WUNNER, *J. Phys. B*, **14** (1981) 751.
- [13] P. SCHMELCHER, L.S. CEDERBAUM and U. KAPPES, *Conceptual Trends in Quantum Chemistry* (Kluwer Academic Publishers) 1994, p. 1-51.
- [14] P. SCHMELCHER, *Phys. Rev. A*, **64** (2001) 063412.
- [15] M. H. BECK *et al.*, *Phys. Rep.*, **324** (2000) .
- [16] G.A. WORTH *et al.*, *The MCTDH Package*, see www.pci.uni-heidelberg/tc/usr/mctdh/.
- [17] V. AVERBUKH *et al.*, *Phys. Rev. A*, **59** (1999) 3695.